



Published in final edited form as:

*Anal Chem.* 2012 May 1; 84(9): 4014–4021. doi:10.1021/ac203330z.

## Compartment modeling for mammalian protein turnover studies by stable isotope metabolic labeling

Shenheng Guan<sup>1,\*</sup>, John C. Price<sup>2</sup>, Sina Ghaemmaghami<sup>2,3</sup>, Stanley B. Prusiner<sup>2,3</sup>, and Alma L. Burlingame<sup>1</sup>

<sup>1</sup>Department of Pharmaceutical Chemistry and Mass Spectrometry Facility, University of California, San Francisco, CA 94158-2517

<sup>2</sup>Institute for Neurodegenerative Diseases, University of California, San Francisco, CA 94143-0518

<sup>3</sup>Department of Neurology, University of California, San Francisco, CA 94143-0518

### SUMMARY

Protein turnover studies on a proteome scale based on metabolic isotopic labeling can provide a systematic understanding of mechanisms for regulation of protein abundances and their transient behaviors. At this time, these large-scale studies typically utilize a simple kinetic model to extract protein dynamic information. Although many high quality, protein isotope incorporation data are available from those experiments, accurate and additionally useful protein dynamic information cannot be extracted from the experimental data by use the simple kinetic models. In this paper, we describe a formal connection between data obtained from elemental isotope labeling experiments and the well-known compartment modeling, and demonstrate that an appropriate application of a compartment model to turnover of proteins from mammalian tissue can indeed lead to a better fitting of the experimental data.

### INTRODUCTION

Quantitative proteomics studies typically provide static comparison of protein abundance differences of the system under study. However, proteins are constantly synthesized and degraded in a living organism depending on their cellular localization and functionality even if their concentrations are kept constant. Although proteins are synthesized by a canonical pathway, protein synthesis rates are subjected to precise transcriptional and translational controls, and influenced by the availability of amino acids. A cell also possesses a number of pathways to remove unwanted protein from the system to modulate the appropriate protein abundances. Abnormal activities of protein degradation pathways have been associated with the onset of numerous diseases. It is likely that all neurodegenerative disorders, including Alzheimer's (AD), Parkinson's, and Huntington's diseases as well as the frontotemporal dementias, may result from the inability of cells to remove the prion forms of etiologic proteins, which subsequently assemble into insoluble aggregates<sup>1</sup>. Understanding the molecular mechanisms of those neurodegenerative diseases may be facilitated by direct measurement of protein turnover in healthy and diseased tissues.

To study protein turnover, it is necessary to apply metabolic isotope labeling methods to trace the amino acid incorporation into a protein. For single-cell organisms, dynamic stable

\*To whom correspondence should be addressed: Shenheng Guan, Mass Spectrometry Facility and Department of Pharmaceutical Chemistry, University of California, San Francisco, 600 16th Street, Genentech Hall, Room N472, Box 2240, San Francisco, CA 94158-2517; sguan@cgl.ucsf.edu.

isotope labeling in culture (dynamic SILAC) experiments<sup>2-4</sup> utilize a single or a few isotopically labeled amino acids to measure protein turnover on a proteome scale. The abundance ratio of labeled and unlabeled peptide ions can be directly used to construct peptide incorporation curves. The free amino acid cytosolic pool in cell cultures can be primed readily with the isotope labels by changing the growth media and the unlabeled amino acids produced by degradation can be quickly diffused into the labeled media. The protein turnover kinetics typically follows a simple exponential mechanism. It is expected that protein turnover in a complex organism, such as a mammal, has much more complicated kinetics.

Recently, we have traced the global protein turnover in mammalian tissues by use of <sup>15</sup>N stable isotope labeling and high resolution mass spectrometry detection<sup>5</sup>. Unlike typical dynamic SILAC experiments, all nitrogen atoms in the food source are labeled with the heavy nitrogen isotope. The advantages of using <sup>15</sup>N labeling include easy production of a natural food source (blue-green algae; *Spirulina platensis*) for mammalian models with near purity of heavy isotope and high dynamic range of isotope incorporation measurement. A disadvantage of the single-element labeling compared to the single amino-acid labeling is that more sophisticated data processing software is needed to extract protein turnover information from complex spectra containing many isotopic peaks. A data processing platform that fulfills this requirement has been described elsewhere<sup>6</sup>. Using a combination of careful execution of optimized experimental protocols and robust data processing algorithms, we were able to measure protein turnover rate constants for ~1700 proteins in mouse tissues. In order to obtain global proteome dynamics in the mammalian samples, we used a simple empirical kinetic model to capture the essence of protein turnover in different tissues. A delayed exponential function was proposed to describe the simple kinetic model<sup>7</sup>. The delay time parameter was included to account for the delay in delivering amino acids from the digestion of the food source. Although the simple kinetic model or the simple model functional form of amino acid incorporation curve fits the general structure of the peptide/protein incorporation curves, there are discrepancies in details of the experimental data so that the simple functional form cannot fit well. In this contribution, we describe the use of more sophisticated compartment kinetic models in an attempt to explain the observed discrepancies. Although the concept of compartment modeling for protein turnover was developed in 1950s<sup>8,9</sup>, we have not found adequate literature providing a clear description for its applications to large-scale dynamic proteomics studies. Here, we attempt to establish a consistent relationship between the experimentally observed data with a compartment model with minimal parameters. The newly developed compartment models can provide the functional forms that can be used for more satisfactory fitting to experimentally observed protein incorporation curves, compared to the simple, widely used one-exponential function.

## THEORY

### One-compartment model

Before examining compartment models for isotope labeling of proteins, we investigated the kinetic information that can be extracted from compartment modeling by measuring relative concentration of labels (Figure 1). In the one-compartment model shown in Figure 1, let  $R_A$  be the flow rate of pure label  $A$  into a compartment (or a pool) initially containing no label, with a volume of  $V$ , starting at  $t=0$ . There are two key assumptions of our current compartment modeling. The first assumption is that a label mixes instantly in a compartment. The second assumption is the size of a compartment does not change during the experiment. In the model, the same volume of mixed material must flow out of the compartment. The concentration of label,  $[A]$ , in the compartment can be described by the differential equation

$$\frac{d[A]}{dt} = \frac{R_A}{V}([A]_T - [A]) \quad (1)$$

in which  $[A]_T$  is the concentration of pure label A. If we measure the relative concentration of A in the compartment, the above equation becomes

$$\frac{d\alpha}{dt} = \frac{R_A}{V}(1 - \alpha) \quad (2)$$

in which  $\alpha = \frac{[A]}{[A]_T}$  is the relative (or fractional) concentration of label A. The solution of the equation is

$$\alpha(t) = (1 - e^{-\frac{R_A}{V}t}) \quad (3)$$

Therefore, the rate constant,  $k_A = \frac{R_A}{V}$ , is the relative volumetric flow rate of label A and the rate constant is inversely proportional to the size of the compartment. This derivation highlights a limitation of an experiment based on measurement of relative concentration of labels. Independent experiments must be carried out in order to obtain independent information about mass or volumetric flow rates or the sizes of compartments.

### Two-compartment model of isotope labeling

We now consider  $^{15}\text{N}$ -labeled amino acids in a two-compartment model (Figure 2). We assign

[AA] as the total concentration of amino acids in the free amino acid pool,

[P] as the total concentration of amino acid in the protein-bound pool,

$V_{AA}$  as the volumetric size of the free amino acid pool,

$V_P$  as the volumetric size of the protein-bound pool,

[ $^{14}\text{NAA}$ ] as the concentration of  $^{14}\text{N}$  amino acid in the free amino acid pool,

[ $^{15}\text{NAA}$ ] as the concentration of  $^{15}\text{N}$  amino acid in the free amino acid pool,

[ $^{14}\text{NP}$ ] as the concentration of  $^{14}\text{N}$  amino acid in the protein-bound pool, and

[ $^{15}\text{NP}$ ] as the concentration of  $^{15}\text{N}$  amino acid in the protein-bound pool.

The model neglects the contribution of the breakdown of a protein of interest into the free amino acid pool because an individual protein's contribution is likely to be small. Assume at time  $t=0$ ,  $^{14}\text{N}$  food source is replaced by  $^{15}\text{N}$  food source with constant amino acid influx of  $R_a$ . According to the model, the following equations can be established for  $^{14}\text{N}$  amino acid

$$V_{AA} \frac{d[^{14}\text{NAA}]}{dt} = -(k_s' + k_{0a}') [^{14}\text{NAA}] \quad (4)$$

$$V_P \frac{d[^{14}\text{NP}]}{dt} = k_s' [^{14}\text{NAA}] - k_b' [^{14}\text{NP}] \quad (5)$$

and for  $^{15}\text{N}$  amino acid

$$V_{AA} \frac{d[15NAA]}{dt} = - (k_s' + k_{0a}') [15NAA] + Ra[AA] \quad (6)$$

$$V_P \frac{d[15NP]}{dt} = k_s' [15NAA] - k_b' [15NP] \quad (7)$$

Under a homeostatic condition (compartment sizes are constant), the total concentration of the free amino acid pool [AA] and that for the protein-bound pool [P] are constants

$$[14NAA] + [15NAA] = [AA] \quad (8)$$

$$[14NP] + [15NP] = [P] \quad (9)$$

We can derive the following relationship due to mass conservation

$$Ra = k_{0a}' + k_s' \quad (10)$$

by use of Equations 4 and 6 and

$$\frac{[AA]}{[P]} = \frac{k_b'}{k_s'} \quad (11)$$

by use of Equations 5 and 7. The differential equations 4–7 are also subjected to the initial conditions (the experimental procedure)

$$[15NAA]_{t=0} = 0 \quad (12)$$

$$[15NP]_{t=0} = 0 \quad (13)$$

Equations 5 and 7 can be combined to give introduction of the following variables

$$\alpha = \frac{[15NAA]}{[AA]} \quad (14)$$

$$\beta = \frac{[15NP]}{[P]} \quad (15)$$

and transforms Equations 6 and 7 into

$$\frac{d\alpha}{dt} = -k_0\alpha + k_0 \quad (16)$$

$$\frac{d\beta}{dt} = k_b\alpha - k_b\beta \quad (17)$$

with the initial conditions of

$$\alpha(0) = 0 \quad (18)$$

$$\beta(0)=0 \quad (19)$$

in which  $k_0 = \frac{k_s' + k_0'}{V_{AA}}$  is the lumped rate constant for amino acid removal from the free amino acid pool and  $k_b = \frac{k_b'}{V_p}$  is the protein degradation rate constant. Just as illustrated in the one-compartment model, it is clear that those rate constants are the relative volumetric flow rate constants normalized by their respective compartment volume sizes. The solution of Equation 16 is an exponential decay function and the solution of Equation 17 is that driven by the exponential decay. Equations 16–17 can be easily solved by use of Laplace transform and the solution of interest as

$$\alpha(t) = e^{-k_0 t} \quad (20)$$

$$\beta(t) = 1 + \frac{k_b e^{-k_0 t}}{k_0 - k_b} - \frac{k_0 e^{-k_b t}}{k_0 - k_b} \quad (21)$$

The half-life times for the free amino acid pool and the protein pool can be found as  $\ln(2) / k_0$  and  $\ln(2) / k_b$ , respectively. Depending on the compartment model and where the label concentrations are measured, some parameters cannot be uniquely determined. The investigation of whether parameters can be determined is called identifiability analysis<sup>8</sup>. In this model, we should be able to extract protein degradation and free amino acid removal rate constants by measuring the amino acid relative concentration in the protein-bound pool alone ( $\beta$ ).

### Relationship between compartment models and experimental data

Now, we need to establish a connection between the relative <sup>15</sup>N-labeled amino acid concentration in protein ( $\beta$ , Equation 15) and the experimentally observed data. Each amino acid contains at least one nitrogen atom; some amino acids contain two (asparagine, glutamine, lysine, and tryptophan), three (histidine), or four (arginine) nitrogen atoms. The relative concentration of <sup>15</sup>N-labeled amino acid in a peptide is proportional to the relative concentration of <sup>15</sup>N atoms in the peptide if all amino acids incorporate into proteins with the same probability. This is, of course, an approximation because there is some delay for non-essential amino acids to become available compared to the essential amino acids. The proportional constant is 1.3577 for an average<sup>10</sup>. The proportional constant cancels out when computing the relative fractional concentration (Equation 15). In our data processing pipeline<sup>6</sup>, we computed the <sup>15</sup>N distribution for every peptide ion identified by a database search. An <sup>15</sup>N distribution is the relative fraction of the peptide ion containing a certain number of <sup>15</sup>N atoms.

Let  $F = \{f_{ij}\}$  be the <sup>15</sup>N distribution matrix, in which row index  $i=1, 2, \dots, NIT$  is the incorporation time points and column index  $j=0, 1, \dots, NNA$  is the number of <sup>15</sup>N atoms incorporated.  $j=0$  corresponds to the peptide with zero <sup>15</sup>N incorporation and  $j=NNA$  is the maximal <sup>15</sup>N incorporation number. The <sup>15</sup>N distribution, of a given incorporation time point  $i$ , is converted to relative <sup>15</sup>N fraction in the peptide by

$$RF_i = \left( \sum_{j=0}^{NNA} \left( \frac{j}{NNA} \right) \frac{f_{ij}}{\sum_{j=0}^{NNA} f_{ij}} \right) \quad (22)$$

The number  $NNA$  is the possible nitrogen atoms that can be metabolically labeled.  $\frac{j}{NNA}$  is the relative ratio of  $^{15}\text{N}$  isotopes over the total exchangeable nitrogen atoms. The  $\frac{f_{ij}}{\sum_{j=0}^{NNA} f_{ij}}$  can be considered as the probability of the peptide ion having  $j$  number of  $^{15}\text{N}$  atoms. The relative fraction of  $^{14}\text{N}$  is simply  $1 - RF_i$ , for the incorporation time point  $i$ . In this work, a peptide incorporation curve is the function of the relative  $^{15}\text{N}$  fraction,  $RF$  against the incorporation time.

### Three-compartment model

As described in the *Results* section, the two-compartment model fit the peptide/protein incorporation relative fraction curves well for proteins in mouse brain. However, the two-compartment model fit poorly to proteins in the liver. An examination of the relative fraction incorporation curves from liver protein revealed that the curves cannot be fitted well even with the general two-exponential functions (see *Results* section for detailed discussion). Therefore, we added an additional total protein compartment to construct a three-compartment model, shown in Figure 3.

The inclusion of the total protein pool is justified because the amino acid recycling by protein degradation and protein export in liver must be considered. The detailed derivation of the three-pool model functional form is given in the supplemental material. A full three-compartment model accounting for both total protein export and total protein degradation (illustrated in Figure S1 of the supplemental material) requires definition of five rate constants. However, we found the fitting of the five-parameter system was not robust because the optimization procedure can easily be trapped in a local minimum. The value for the rate constants for both the total protein degradation into free amino acid ( $k_{bt}$ ) and the total protein export ( $k_{ot}$ ) should be small because they are normalized by the large volumetric size of the total protein pool. Indeed, the five-rate constant values for good fits showed that the total protein export rate constant was typically the smallest one. Thus, we removed the rate constant for total protein export from consideration in order to reduce the degree of parametric dimension, resulting in a four-rate constant system (Figure 3). The relative concentration of  $^{15}\text{N}$ -labeled amino acid in each protein of interest is

$$\gamma(t) = 1 + y_u e^{-ut} + y_\nu e^{-\nu t} + y_{k_{bt}} e^{-k_{bt}t} \quad (23)$$

in which

$$u = \frac{(k_{st} + k_{0a} + k_{bt}) - \sqrt{(k_{st} + k_{0a} + k_{bt})^2 - 4k_{0a}k_{bt}}}{2} \quad (24)$$

$$\nu = \frac{(k_{st} + k_{0a} + k_{bt}) + \sqrt{(k_{st} + k_{0a} + k_{bt})^2 - 4k_{0a}k_{bt}}}{2} \quad (25)$$

$$y_u = \frac{k_{0a}k_{bi}(u - k_{bt})}{(u - \nu)(u - k_{bi})u} \quad (26)$$

$$y_\nu = \frac{k_{0a}k_{bi}(\nu - k_{bt})}{(\nu - u)(\nu - k_{bi})\nu} \quad (27)$$

$$y_{k_{bt}} = \frac{k_{0a}(k_{bi} - k_{bt})}{(u - k_{bi})(\nu - k_{bi})} \quad (28)$$

The solution contains three exponentials. A general form of three-exponential function ( $y(t) = 1 + y_1e^{-k_1t} + y_2e^{-k_2t} + y_3e^{-k_3t}$ ) requires six parameters for its definition. Here only four parameters— $k_{st}$ , total protein synthesis rate constant;  $k_{bt}$ , total protein degradation rate constant;  $k_{0a}$ , amino acid out flow rate constant;  $k_{bi}$ , individual protein degradation rate constant—completely define our three-compartment model. In other words, the system has four degrees of parametric freedom. When the function was used to fit the experimental incorporation curves, the fitness was similar to the fittings with the full five-parameter function containing the total protein export rate constant.

## RESULTS

All data are from experiments previously described<sup>7</sup>. The data processing for the <sup>15</sup>N distribution of peptide ions was described<sup>6</sup>. Fitting the compartment model functional forms using <sup>15</sup>N distribution data was done similarly as described<sup>6</sup>. Briefly, the relative <sup>15</sup>N fraction was calculated according to Equation 22 and the peptide incorporation curves were constructed from the relative <sup>15</sup>N fraction data points against the incorporation times. The relative <sup>15</sup>N fraction incorporation curves of the peptide ions belonging to a protein were aggregated to the protein <sup>15</sup>N incorporation curve by use of a similarity selection procedure after the shared peptides were removed. In order to guarantee the quality of the protein incorporation curves, we only considered the curves obtained by aggregation of at least two peptide curves and that contained at least four nonzero data points out of nine incorporation times. Still, there were 705 and 797 protein curves to consider in brain and liver, respectively. The supplemental material contains the protein <sup>15</sup>N relative fraction incorporation curves along with the fitted rate constants.

### Relative isotope fraction

As discussed in the theoretical section, relative <sup>15</sup>N fraction (substituting for <sup>15</sup>N-labeled amino acid concentration) provides a direct connection of compartment models to the experimental observation. An additional advantage of using relative isotope fraction instead of the commonly used relative isotope abundance (RIA) is illustrated in Figure 4. For proteins with rapid turnover, the incorporation curves using relative isotope abundance (RIA) can quickly reach saturation. This is quite common for many proteins in liver (Figure 4, upper right). In comparison, no proteins attain saturation with the incorporation curves using relative isotope fraction (Figure 4, lower panels).

### Brain proteins: two-compartment modeling

The relative <sup>15</sup>N fraction incorporation curves for brain proteins were subjected to a nonlinear regression procedure to fit the theoretical function of Equation 21 for the two-compartment model. Compared to the empirical delayed exponential function ( $\beta(t) =$

$1 - e^{-k_0(t-t_0)}$ , for which  $k_0$  is the rate constant and  $t_0$  is the time delay) to fit the relative isotope abundance proposed in<sup>7</sup>, the two-compartment function fit better for almost all of the 700 protein relative fraction incorporation curves from brain although both models use two fitting parameters (Figure 5).

Shown in Figure 5 are two curve fittings of the same protein (phosphatidylethanolamine-binding protein 1, P70296). The fitting was much more precise for the two-compartment model (Figure 5, lower trace). The rate constant obtained from the two-compartment model ( $0.0373 \text{ day}^{-1}$ ) is approximately 40% smaller than that of  $0.0563 \text{ day}^{-1}$  from the delayed exponential fit (Figure 5, upper trace).

The improvement in fitting of the two-compartment model over the delayed exponential function for all the selected brain proteins is illustrated in Figure 6. The majority (>70%) of the two-compartment model fitting had R2 values of 0.99 or better. In the case of the delayed exponential fit, a smaller portion (<40%) can be fitted equally or better.

It is interesting to examine the extreme cases of the functional form of Equation 21. If the protein degradation rate constant,  $k_b$ , is much smaller than the amino acid removal constant  $k_0$ , or  $k_b \ll k_0$  the solution (Equation 21) reduces to a single exponential function (one compartment).

$$\beta(t) \approx 1 - e^{-k_b t} \quad (29)$$

One additional disadvantage for using the delayed exponential function is the sensitivity of the fit with early incorporation time points. If the delay factor is positive, the delayed exponential function becomes negative when the incorporation time is small. This is, of course, inconsistent with the definition of relative isotope abundance, which should have a possible range from zero to one. One can consider eliminating the early incorporation time points; however, such a choice is subjective and a data processing procedure based on such input is not robust.

Any nonlinear fitting requires an initial parametric value. The fitting of the two-compartment model is robust. For all the protein curves tested, the fitting converged to the global minimum with the same initial values for both rate constants. It is perhaps not surprising here because there are only two degrees of parametric freedom in this system.

### Liver proteins: three-compartment modeling

When attempting to fit the  $^{15}\text{N}$  relative fraction incorporation curves for liver proteins with the two-compartment model function of Equation 21, a high degree of deviation was observed (Figure 7). In fact, the two-compartment model fitted more poorly than the delayed exponential function, which is equivalent to a general one-exponential function ( $1 - y_0 e^{-kt}$ , in which  $y_0$  and  $k$  are the fitting parameters). Using a general two-exponential function ( $\gamma(t) = 1 + y_1 e^{-k_1 t} + y_2 e^{-k_2 t}$  with four parameters) did not produce better fitting (data not shown). Introduction of the third total protein compartment produced much-improved fitting for most proteins in liver, even when the number of the fitting parameters was kept at four. A typical example is shown in Figure 8, in which the  $^{15}\text{N}$  relative fraction incorporation curve for the protein transitional endoplasmic reticulum ATPase (Q01853) was constructed from 37 of its peptide incorporation curves. In a liver protein turnover study with  $^{14}\text{C}$  labeling<sup>11</sup>, a three-exponential function was found to be more appropriate.

The two-compartment model fitted poorly with the protein degradation rate constant of  $0.137 \text{ day}^{-1}$  and the three-compartment model fitted nearly perfectly with the data for the protein degradation rate constant of  $0.317 \text{ day}^{-1}$ . It is interesting to note that the total protein



degradation rate constant ( $k_{bt}$ ) is very small. This perhaps should not be surprising because the total protein pool size is very large compared to that for free amino acids in a tissue as discussed for the single-compartment model. The statistical analysis of all total protein degradation rate constants for liver proteins support this statement (Figure 9). The median value of the total protein degradation rate constants for all the liver proteins was approximately  $0.04 \text{ day}^{-1}$ , which is at least one order of magnitude smaller than the other rate constants. Many total protein degradation rate constants had negative values. Of course, these negative values cannot be correct. From an experimental point of view, this can be explained by a situation in which the variation caused by observation errors is larger than the expected values.

## DISCUSSION

In the theoretical section, we introduced a series of compartment models with increasing sophistication in order to fit the experimentally observed data better. The most important development here is the realization that the relative isotopically labeled fraction can serve as a direct connection between compartment modeling and the experimental data. The relative isotope fraction can be accurately extracted from a single survey scan spectrum from its isotopic peaks without the need to introduce an external factor for its normalization. In a typical dynamic SILAC experiment, if the detected peptide contains a single labeled amino acid, the relative isotope abundance is equal to the relative fraction concentration. However, if the peptide of interest contains more than one labeled amino acid, the relative isotope fraction is a more appropriate indication of the relative amino acid concentration of the peptide instead of the relative isotope abundance.

In a typical large-scale protein turnover study, a large number of high quality protein incorporation curves are available because each can be constructed by use of many (sometimes hundreds) peptide incorporation curves. The compartment models presented here seem able to provide optimal functional forms for fitting the experimental data. For brain proteins, the two-compartment model with only two parameters provided superior fitting compared to any two-parameter functional forms with single compartment models, demonstrating the importance of the correct functional forms. For liver proteins, we attempted to produce a three-compartment model with a minimal number of parameters. A more general three-compartment model with five rate constants, including that for total protein export, is described in the supplemental material. But with the five-parameter system, it was difficult to produce satisfactory fits to the experimental data because it is more sensitive to the initial parameter estimates. The four-parameter system was more robust and produced substantial improvement over the less sophisticated models.

We have also compared the rate constants obtained by fitting relative isotope fraction with compartment modeling against those from fitting relative isotope abundance with the empirical delayed exponential function (see supplemental Figures S1 and S2). In general, the correlations were strong and the ranking order of magnitude was kept in the two data sets. Therefore, the functional analysis given previously<sup>7</sup> remains valid. But the values of the rate constants do differ. For brain proteins, the range and values of  $k_{bs}$  from the two-compartment model were smaller than those from the delayed exponential fit. This may result from the reduction of outliers in the two-compartment modeling, which separates the contribution of the amino acid removal better than the simple delayed exponential model. This effect was more dramatic for the liver proteins. For the majority of the liver proteins, the individual protein degradation rate constants exhibited a wider range. The delayed exponential modeling seems incapable of accurately extracting individual degradation rate constants with small values for liver proteins. The compartment modeling by use of the relative amino acid concentration (proportional to the relative isotope fraction) has a

disadvantage of being unable to separate the compartment size from its rate constant. For example, under the present modeling framework, a small relative isotope fraction can result from either a small portion of completely labeled proteins or all proteins labeled with a small level of labeling. Additional theoretical and informatics development is needed to explain the two extreme cases.

## Supplementary Material

Refer to Web version on PubMed Central for supplementary material.

## Acknowledgments

This work was supported by NIH NCRR grants RR01614 (to ALB), RR019934 (to ALB), NIH grants AG010770 (to SBP) and AG021601 (to SBP) as well as gifts from the G. Harold and Leila Y. Mathers Charitable Foundation and the Sherman Fairchild Foundation.

## ABBREVIATIONS

<b>RIA</b>	Relative isotope abundance
<b>SILAC</b>	Stable isotope labeling with amino acids in culture
<b>SILAM</b>	Stable isotope labeling of mammals

## REFERENCES

1. Colby DW, Prusiner SB. *Nat. Rev. Microbiol.* 2011; 9:771–777. [PubMed: 21947062]
2. Claydon AJ, Beynon RJ. *Methods Mol Biol.* 2011; 759:179–195. [PubMed: 21863488]
3. Doherty MK, Hammond DE, Clague MJ, Gaskell SJ, Beynon RJ. *Journal of proteome research.* 2009; 8:104–112. [PubMed: 18954100]
4. Pratt JM, Petty J, Riba-Garcia I, Robertson DH, Gaskell SJ, Oliver SG, Beynon RJ. *Mol Cell Proteomics.* 2002; 1:579–591. [PubMed: 12376573]
5. Price JC, Guan S, Burlingame AL, Prusiner SB, Ghaemmaghami S. *Proc. Natl. Acad. Sci. USA.* 2010; 107:14508–14513. [PubMed: 20699386]
6. Guan S, Price JC, Prusiner SB, Ghaemmaghami S, Burlingame AL. *Molecular & cellular proteomics : MCP.* 2011
7. Price JC, Guan S, Burlingame A, Prusiner SB, Ghaemmaghami S. *Proceedings of the National Academy of Sciences of the United States of America.* 2010; 107:14508–14513. [PubMed: 20699386]
8. Carson, ER.; Cobelli, C.; Finkelstein, L. *The Mathematical modeling of metabolic and endocrine systems.* New York: John Wiley & Sons; 1983.
9. Wolfe, RR.; Chinkes, DL. *Isotope Tracers in metabolic Research.* 2nd ed.. Hoboken, New Jersey: John Wiley & Sons; 2005.
10. Senko MW, Beu SC, McLafferty FW. *Journal of the American Society for Mass Spectrometry.* 1995; 6:229–233. [PubMed: 24214167]
11. Garlick PJ, Waterlow JC, Swick RW. *Biochem J.* 1976; 156:657–663. [PubMed: 949347]

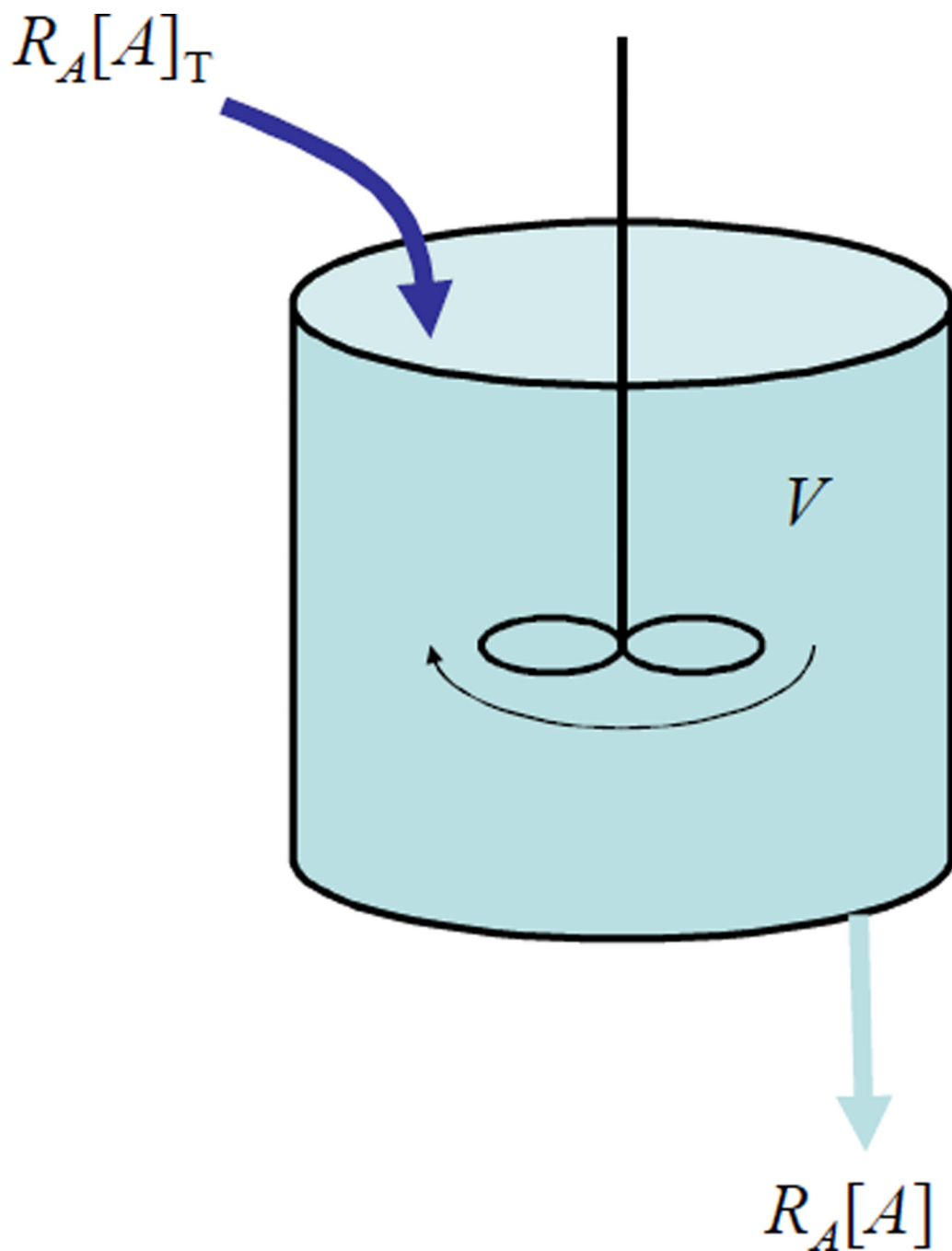


**Figure 1.** One-compartment model.  $R_A[A]_T$  and  $R_A[A]$  are the quantities (moles if the concentrations are in Molar unit and  $R_A$  is in liter per unit time) flowed into and out of the compartment per unit of time, respectively.

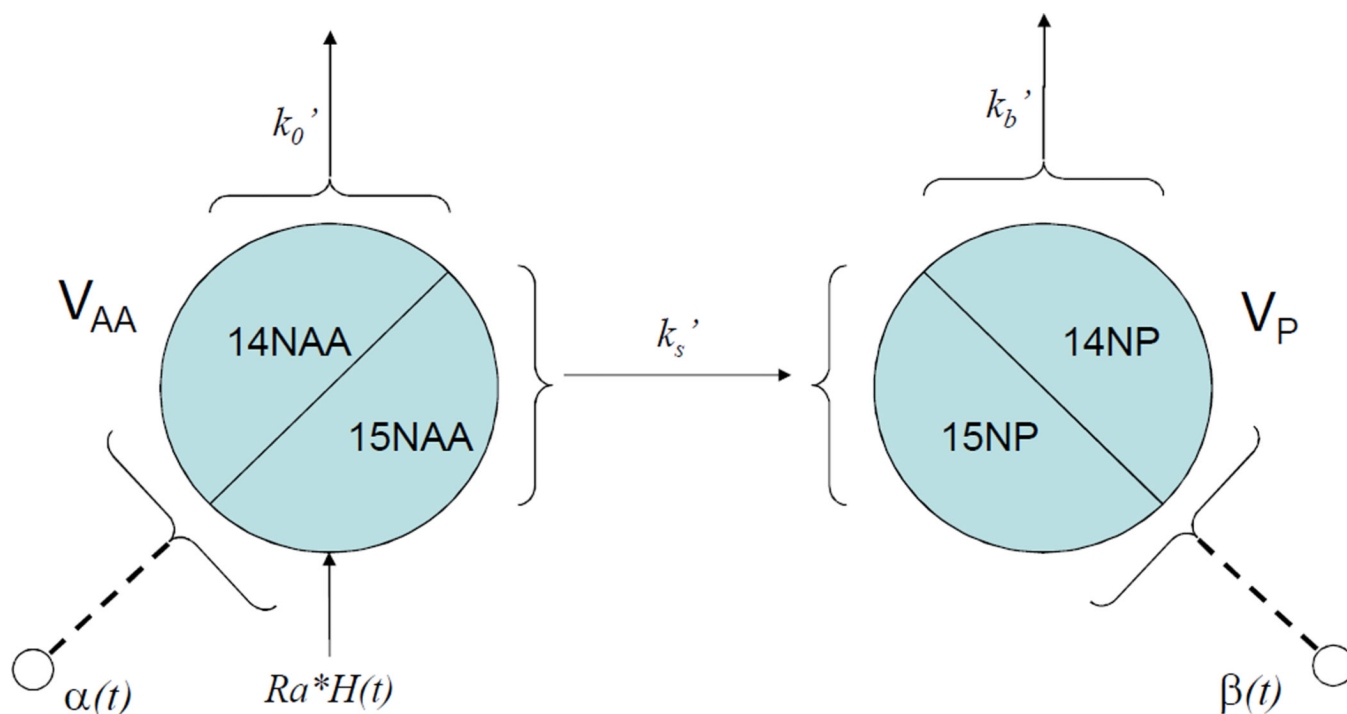


**Figure 2.**

Two-compartment model for protein turnover in brain.  $H(t)$  is the step function of  $t$ ;  $H(t)=0$  for  $t<0$  and  $H(t)=1$  for  $t \geq 0$ .  $V_{AA}$  and  $V_P$  are the volumetric sizes of the free amino acid pool and the protein-bound pool, respectively. Assuming there is not an isotope effect, the rate constants are the same for both unlabeled and labeled amino acids.  $\alpha$  and  $\beta$  are the fractional concentration of  $^{15}N$ -labeled amino acids in the free amino acid pool and the protein-bound pool, respectively.

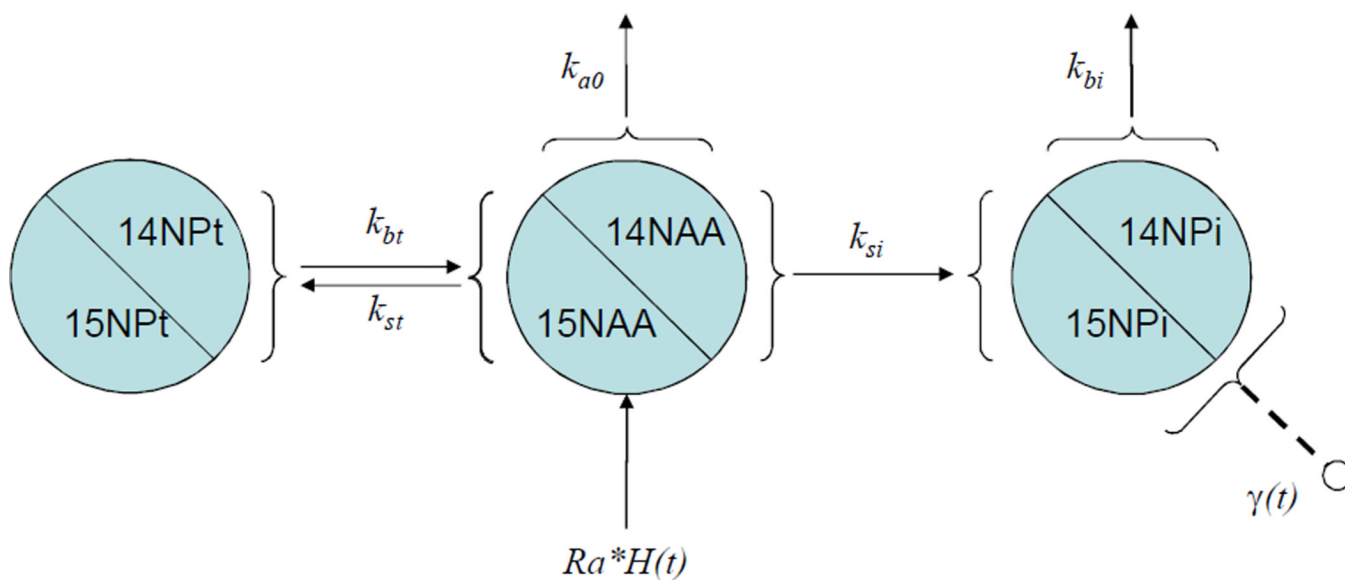


**Figure 3.**

Three-compartment model for protein turnover in liver. The compartments are the free amino acid pool ( $^{14}\text{NAA}/^{15}\text{NAA}$ ), the total protein pool ( $^{14}\text{NPt}/^{15}\text{NPt}$ ), the protein-of-interest pool ( $^{14}\text{NPi}/^{15}\text{NPi}$ ).  $V_{AA}$ ,  $V_{Pt}$ , and  $V_{Pi}$  are the volumetric sizes of the free amino acid pool, the total protein-bound pool, and the individual protein-bound pool, respectively.

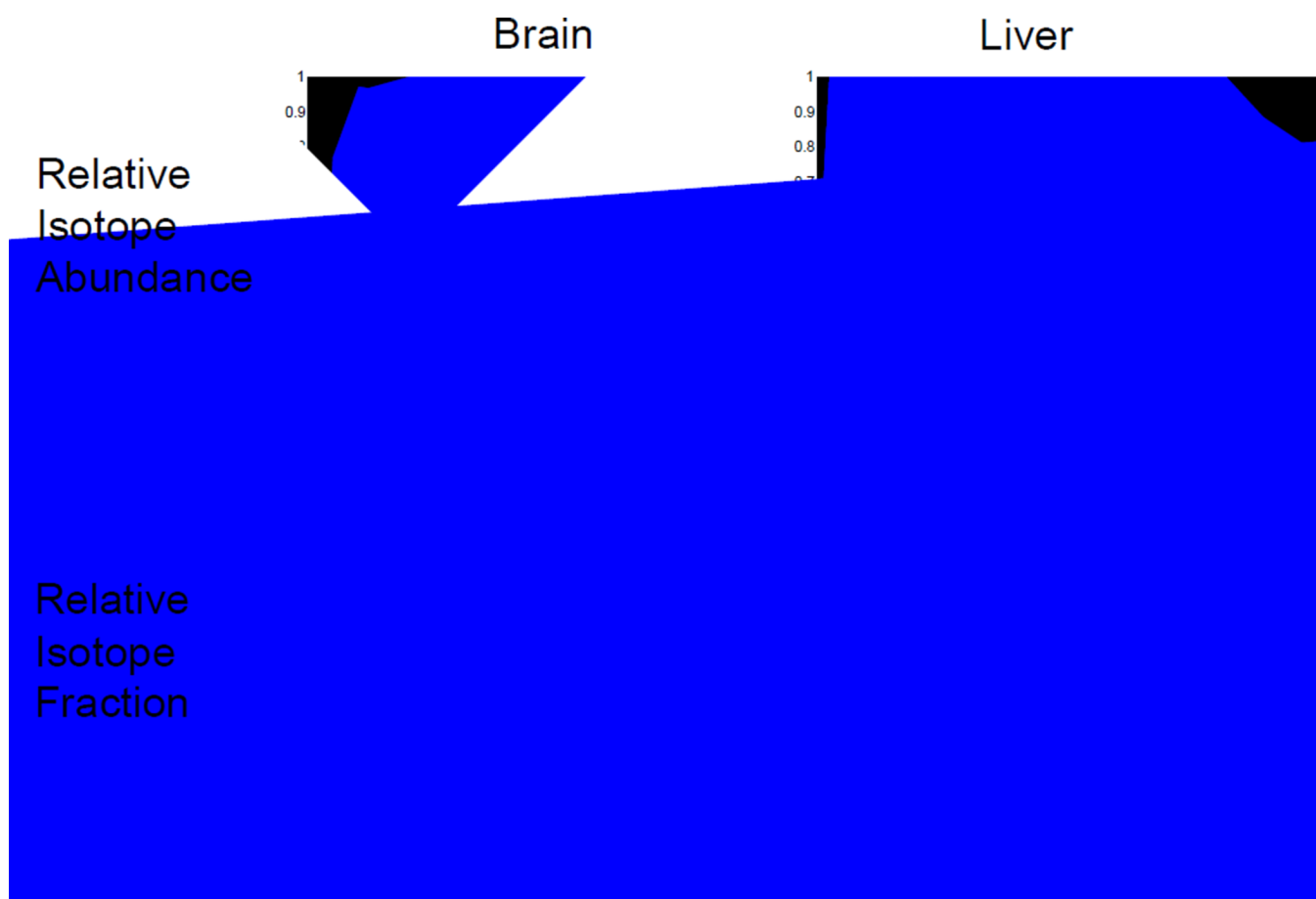


**Figure 4.** Peptide incorporation curves constructed by use of relative isotope abundance (RIA; top panels) or by use of relative isotope fraction, defined by Equation 22 (bottom panels). Peptide curves are from brain proteins (left panels) and from liver proteins (right panels).

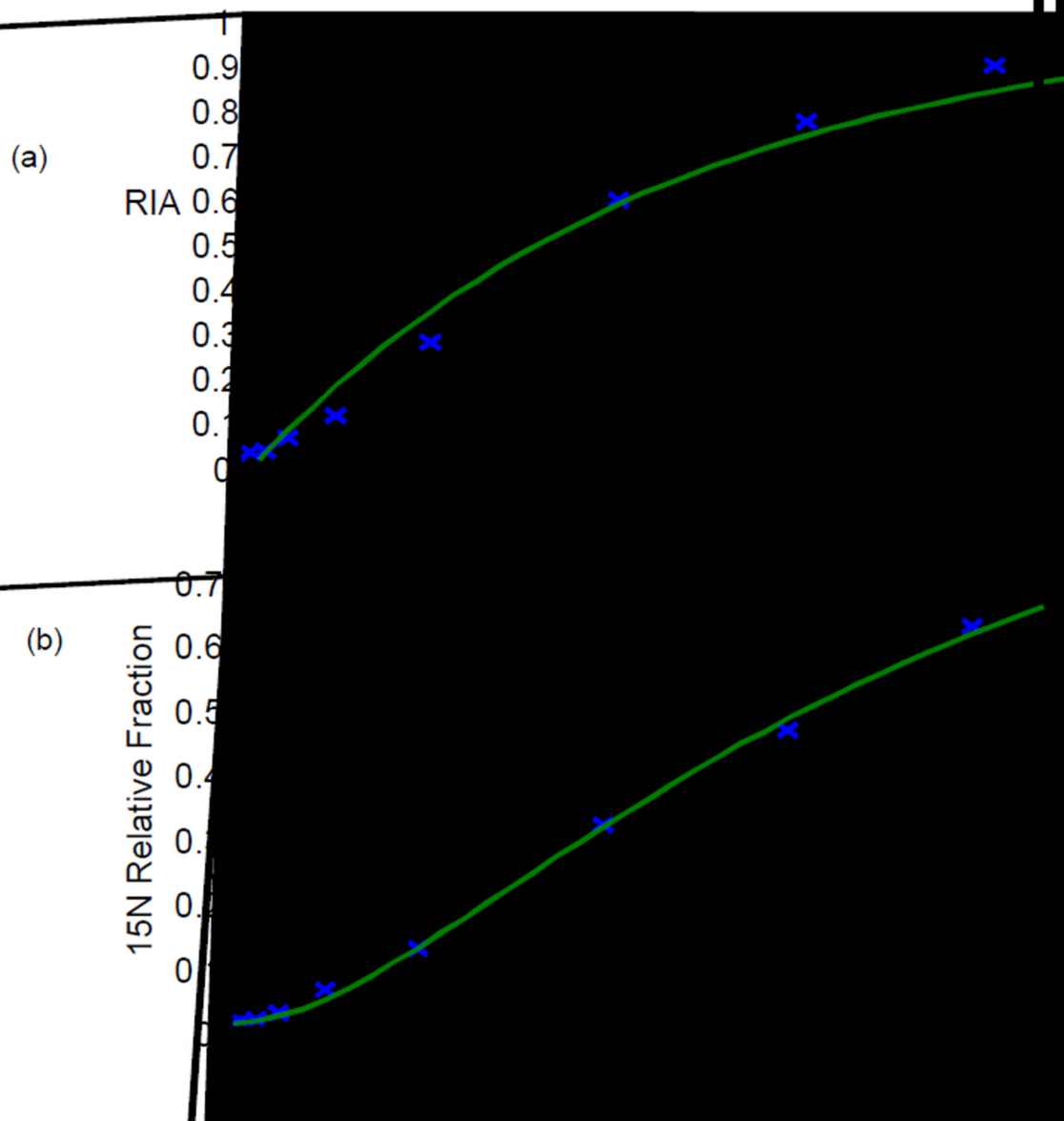


**Figure 5.** Fitting protein incorporation curves by used a delayed exponential function for relative isotope abundance (a) and by use of the two-compartment model function of Equation 21 for relative isotope fraction (b).

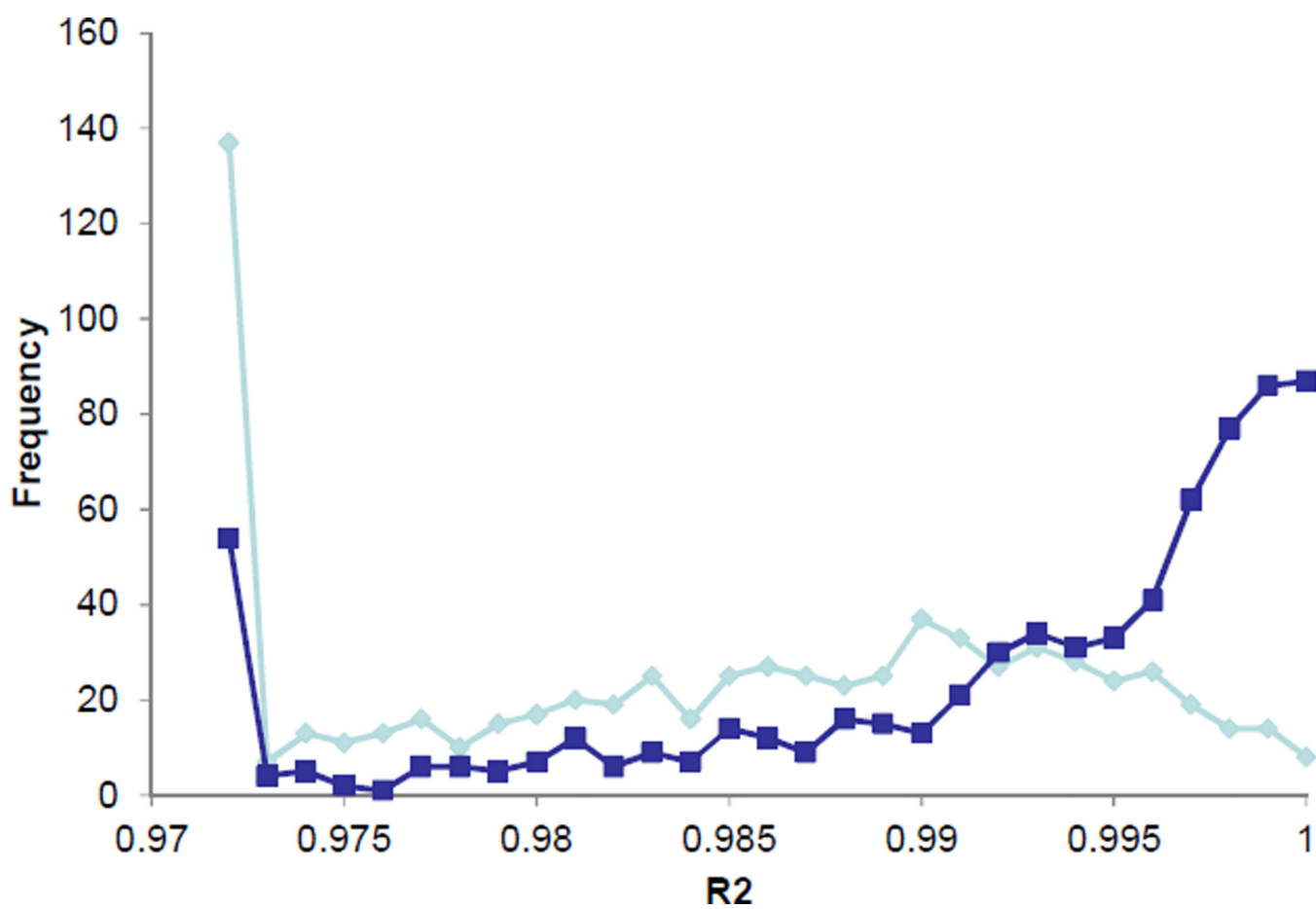


**Figure 6.** Brain protein incorporation curve fitting. Fitness comparison of the delayed exponential function for relative isotope abundance (gray trace) and the two-compartment model function for relative isotope fraction (black trace).



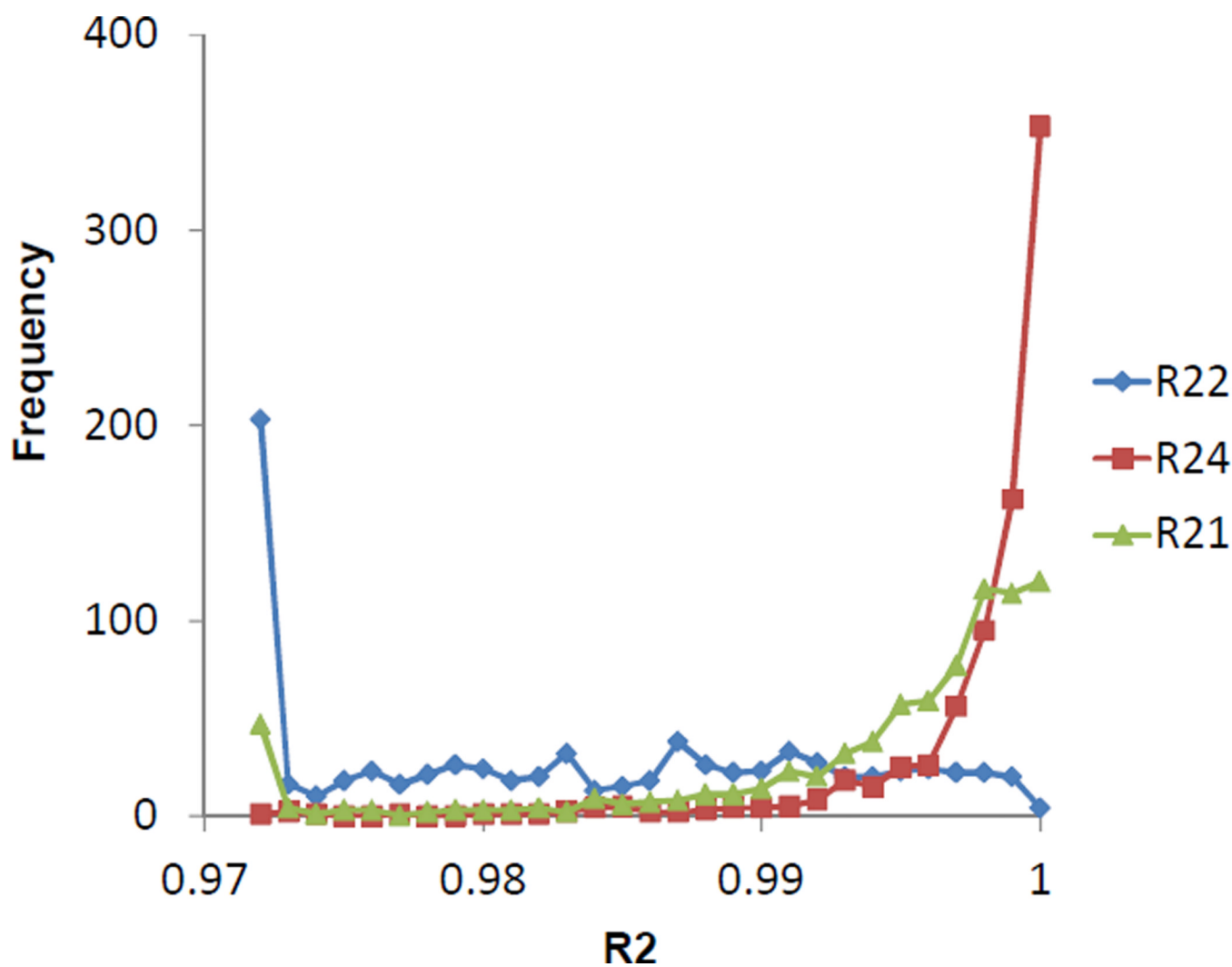


**Figure 7.** Liver protein incorporation curve fitting. Fitness comparison of the delayed exponential function for relative isotope abundance (gold trace,  $R_{21}$ ), the two-compartment model function for relative isotope fraction (blue trace,  $R_{22}$ ), and the three-compartment model function for relative isotope fraction (red trace,  $R_{24}$ ).

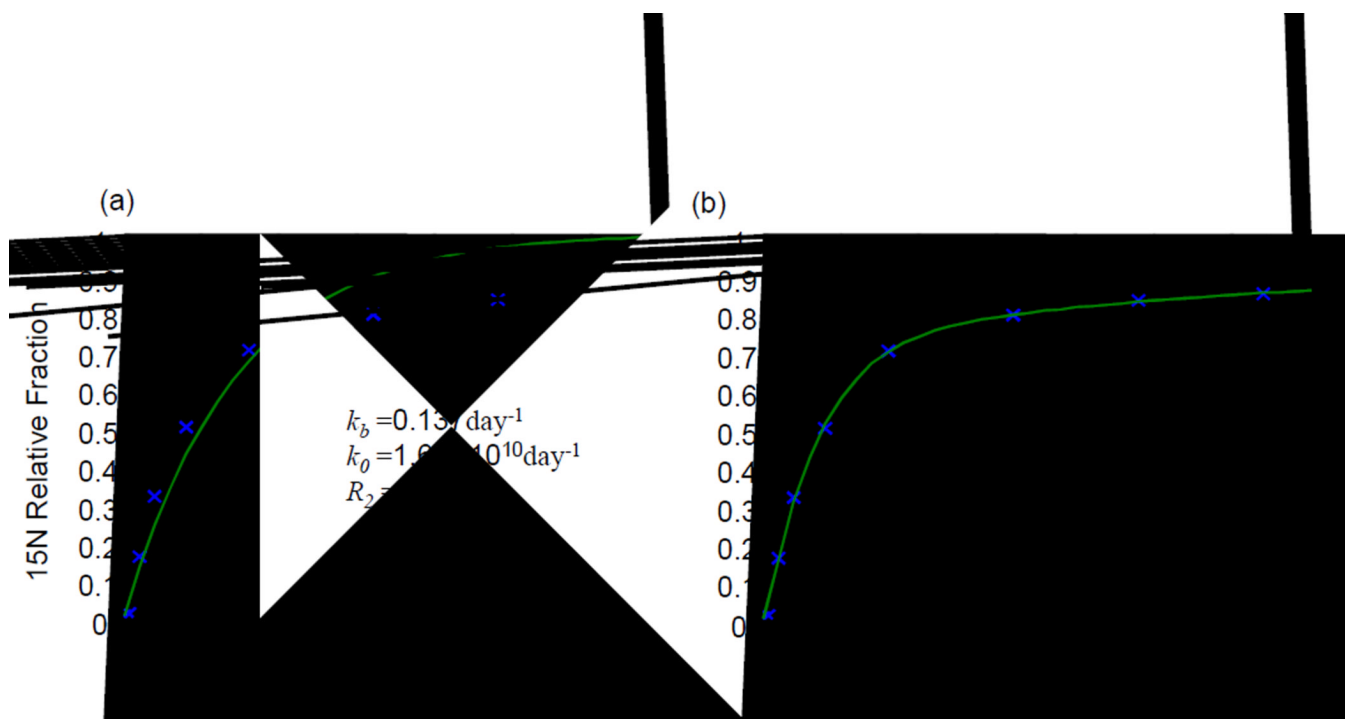


**Figure 8.** Illustration of curve fitting for a liver protein, transitional endoplasmic reticulum ATPase. The two-compartment model function fitting with two rate constants (a), and the three-compartment model function fitting with four rate constants (b).

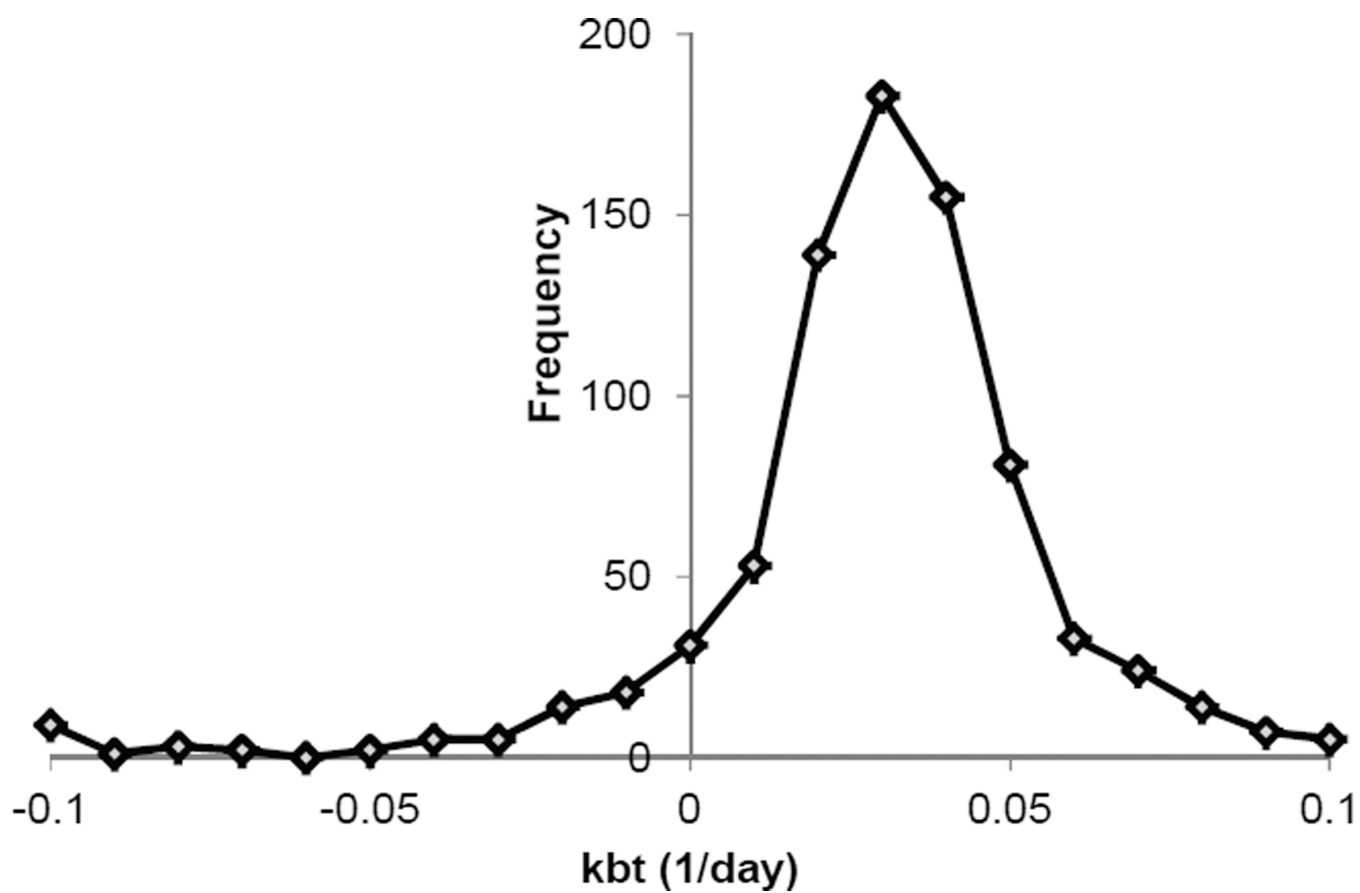


**Figure 9.** Histogram of total protein degradation rate constants obtained by use of the three-compartment model function for fitting relative  $^{15}\text{N}$  fraction incorporation curves of liver proteins.